© 2015. Published by The Company of Biologists Ltd | Development (2015) 142, 3512-3518 doi:10.1242/dev.128157

RESEARCH REPORT

A non-signaling role of Robo2 in tendons is essential for Slit processing and muscle patterning

Elly Ordan and Talila Volk*

ABSTRACT

Coordinated locomotion of an organism relies on the development of proper musculoskeletal connections. In *Drosophila*, the Slit-Robo signaling pathway guides muscles to tendons. Here, we show that the Slit receptor Roundabout 2 (Robo2) plays a non-cell-autonomous role in directing muscles to their corresponding tendons. Robo2 is expressed by tendons, and its non-signaling activity in these cells promotes Slit cleavage, producing a cleaved Slit N-terminal guidance signal that provides short-range signaling into muscles. Consistently, *robo2* mutant embryos exhibited a muscle phenotype similar to that of *slit*, which could not be rescued by muscle-specific Robo2 expression but rather by ectodermally derived Robo2. Alternatively, this muscle phenotype could be induced by tendon-specific *robo2* RNAi. We further show that membrane immobilization of Slit or its N-terminal cleaved form (Slit-N) on tendons bypasses the functional requirement for Robo2 in tendons, verifying that the major role of Robo2 is to promote the association of Slit with the tendon cell membrane. Slit-N tends to oligomerize whereas full-length uncleavable Slit does not. It is therefore proposed that Slit-N oligomers, produced at the tendon membrane by Robo2, signal to the approaching muscle by combined Robo1 and Robo3 activity. These findings establish a Robo2-mediated mechanism, independent of signaling, that is essential to limiting Slit distribution and which might be relevant to the regulation of Slit-mediated short-range signaling in additional systems.

KEY WORDS: *Drosophila* embryo, Muscle, Robo, Slit, Slit cleavage

INTRODUCTION

In both vertebrates and invertebrates, the establishment of a functional musculoskeletal tissue requires a precise encounter between muscles and tendons (Schejter and Baylies, 2010; Schnorrer and Dickson, 2004; Schweitzer et al., 2010; Volk, 1999). Active cross-talk between tendons and elongating muscles has been demonstrated in *Drosophila*, where an important tendon-specific guidance signal is the secreted protein Slit (Kramer et al., 2001; Ordan et al., 2015; Wayburn and Volk, 2009). The contribution of the different Slit receptors, namely Robo1 (also known as Robo), Robo2 and Robo3, to muscle patterning remains elusive. Genetic studies have suggested that Robo1 and Robo2 cooperate in responding to the secreted tendon-specific ligand Slit on the muscle side (Kramer et al., 2001); however, this has never been directly tested.

Slit contains a conserved cleavage site (Brose et al., 1999; Wang et al., 1999). Recently, we showed that, in tendons, full-length Slit (Slit-FL) undergoes cleavage, creating an active, stable N-terminal polypeptide (Slit-N), which associates with the tendon cell surface, thus limiting the range of Slit signaling. Moreover, Slit cleavage at the surface of tendon cells was found to be crucial for short-range muscle repulsion, as well as for providing a stop signal for LT and DA3 muscles (Ordan et al., 2015); however, the molecular mechanism promoting localized Slit cleavage has yet to be elucidated. Here, we show that, for muscle guidance, Robo2 activity is required in tendon cells and not in muscles. Furthermore, Robo2 activity in tendons can promote Slit cleavage, creating the non-diffusible Slit-N; for this function the receptor extracellular domain is sufficient. Slit-N polypeptides were found to oligomerize, and this explains their reactivity with both tendons and muscles. Consistent with the role of Robo2 in muscle directional elongation by limiting Slit diffusion, knocked-in membrane-bound, full-length, uncleavable Slit rescued the muscle phenotype of *robo2* mutants, whereas Slit lacking the membrane domain did not. These findings demonstrate a novel signaling-independent role for Robo2 in facilitating Slit activity in cis, which is important for promoting Slit short-range signaling.

RESULTS AND DISCUSSION

Lack of *robo2* causes a strong muscle phenotype

To determine the individual contribution of Robo family receptors to the embryonic muscle pattern, we analyzed the orientation of the three lateral transverse muscles (LT1-3) and of the dorsal acute muscle 3 (DA3) in *Drosophila* embryos at stage 16 lacking distinct Robo receptors and compared it with that of *slit* mutants. In *slit* mutant embryos, the LT muscles are closer to the posterior segment border and are not spaced correctly, and the DA3 muscle does not extend its leading edge in an orthogonal fashion (Fig. 1A-B′) (Ordan et al., 2015).

The orientation of the LT and the DA3 muscles in *robo1* or *robo3* mutants exhibited almost normal positioning relative to their wild-type (WT) counterparts (Fig. 1C,E,C′,E′). Quantification of the distance of LT3 muscle to the posterior segment border divided by overall segmental width (D_{LT3}/D_s) revealed no significant difference between *robo1* and WT (P=0.8313) or *robo3* and WT (P=0.74) (Fig. 2L). However, in *robo1;robo3* double-mutant embryos the orientation of these muscles resembled that of *slit* mutants (Fig. 1F,F′ and Fig. 2L; P=0.0001). *robo2* mutants exhibited a phenotype that was comparable to that of *slit* mutants; the LT muscles were not equally spaced and were closer to the posterior segmental border, a phenotype observed in 85% of the segments (P=0.0001, n=47) (Fig. 1D). Quantification of D_{LT3}/D_s revealed a smaller value in the *robo2* mutant (0.16 as compared with 0.34 in WT, P=0.0001; Fig. 2L). In addition, in 33% of the *robo2* mutant segments, the DA3 muscle lost its diagonal orientation and often migrated in a straight ventral-dorsal orientation (P=0.0037, n=43; Fig. 1D′).

Department of Molecular Genetics, Weizmann Institute of Science, Rehovot 76100, Israel.

*Author for correspondence (talila.volk@weizmann.ac.il)

Received 4 July 2015; Accepted 1 September 2015

Development (2015) 142, 3512-3518 doi:10.1242/dev.128157

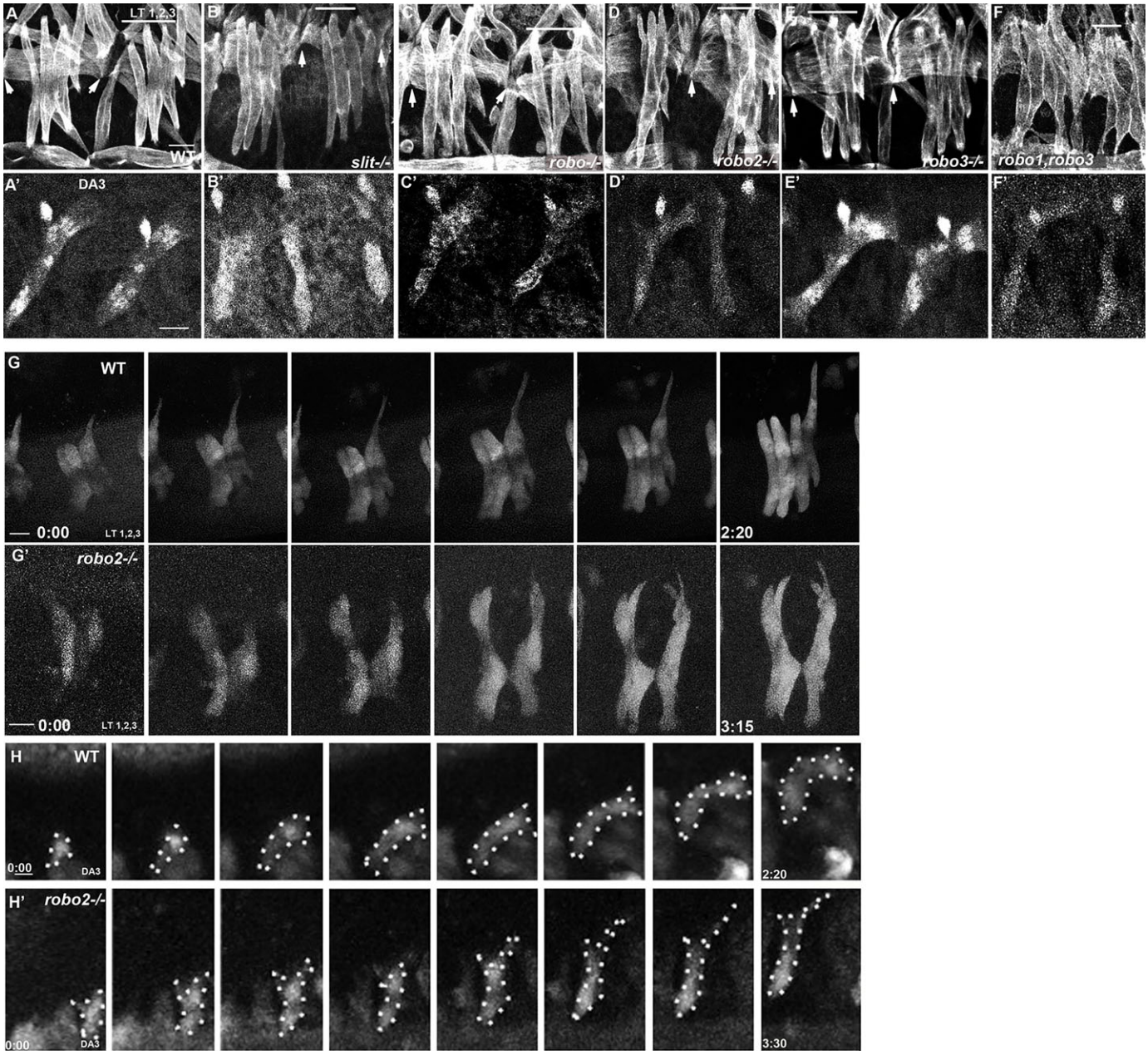

Fig. 1. Robo2 has a major role in patterning embryonic muscles. (A-F′) Wild-type (WT) (A,A′) and *slit* (B,B′), *robo1* (C,C′), *robo2* (D,D′) and *robo3* (E,E′) mutant *Drosophila* embryos and *robo1,robo3* double mutants (F,F′) at stage 16 stained with anti-Tropomyosin (A-F) to visualize the LT muscles or with anti-Collier (A′-F′) to label the DA3 muscle. The horizontal line indicates the span of LT muscles 1-3; arrows point to the segmental border. (G,G′) Time frames from live imaging of WT (G) or *robo2* mutant (G′) LT muscles at stages 13-16, labeled with Ap-Me580-GFP (see also Movies 1 and 2). (H,H′) Time frames of live imaging of WT (H) or *robo2* mutant (H′) DA3 muscles at stages 12-13, labeled with Collier-GFP (dots indicate the muscle outline) (see also Movies 3 and 4). Time is h:min. Scale bars: 10 µm.

To reveal the dynamic nature of the process of muscle elongation in *robo2* mutants, we followed individual muscles in live *robo2* mutant and control embryos using specific GFP-marked LT (Fig. 1G,G′, Movies 1 and 2) or DA3 (Fig. 1H,H′, Movies 3 and 4) muscles at stages 13-16 throughout muscle elongation. This analysis showed that the polarity of the mutant muscles was similar to that of WT control muscles; however, the LT muscles tended to elongate closer to the segment border and were not evenly spaced. The DA3 muscle often did not turn towards the posterior segment, and both muscles reached their target tendons more slowly. These results suggested differential contributions of the Robo receptors to the directed elongation of LT and DA3 muscles.

Robo2 acts non-autonomously in directing muscle elongation

To reveal the relative distribution and expression levels of the Robo receptors in muscles, we took advantage of flies carrying an HA tag that was knocked-in within the genomic region of each of the Robo receptors (Spitzweck et al., 2010), and labeled embryos with anti-HA. Robo1-HA accumulated at the muscle-tendon junction (open arrow) and was observed at low levels on the muscle surfaces (white arrow) (Fig. 2A). Robo2 levels were prominent along ectodermal stripes (open arrow) but not on muscles (Fig. 2B), and Robo3 labeling was indistinguishable from background (Fig. 2C). Double labeling with anti-Robo2 and anti-Stripe (Sr) (Fig. 2D-F) or with

Development (2015) 142, 3512-3518 doi:10.1242/dev.128157

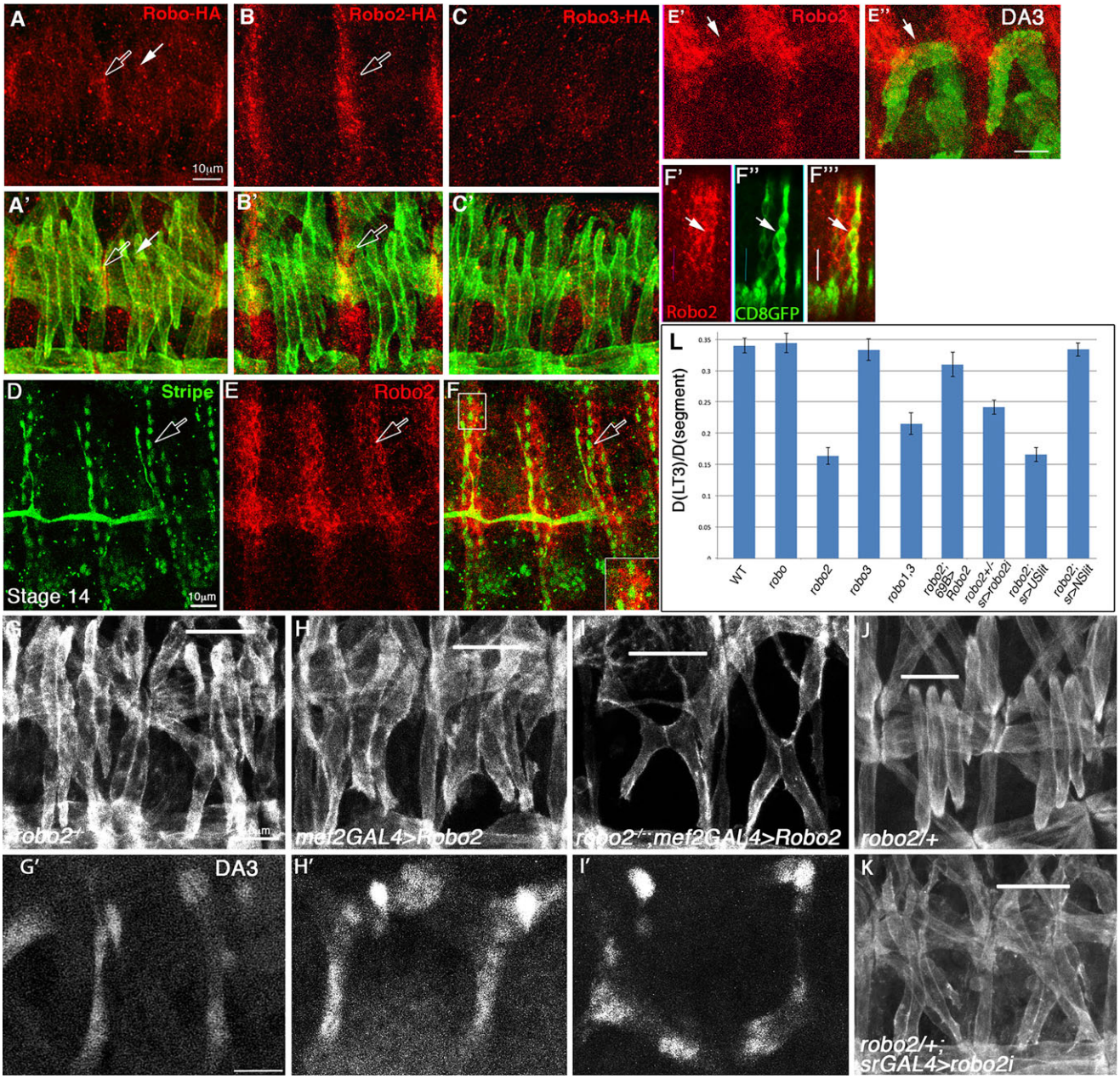

Fig. 2. Robo2 affects the LT and DA3 muscles non-cell-autonomously. (A-C′) Embryos at stage 16 carrying an HA tag in the genomic locus of either *robo1* (A,A′), *robo2* (B,B′) or *robo3* (C,C′) labeled with anti-HA (red) and anti-Tropomyosin (green). Open arrow in A,A′ indicates the edge of the muscle; white arrow indicates muscle surfaces. Open arrow in B,B′ indicates the ectodermal stripe. (D-F) Robo2 expression in tendon cells of WT embryos at stage 14, labeled with anti-Stripe (green) and anti-Robo2 (red). Open arrow indicates tendon cells. The boxed region in F is magnified in the inset. (E′,E″) WT embryo expressing Collier-GFP and labeled with anti-Robo2. Arrow indicates Robo2 distribution at the border of the DA3 diagonal path. (F′-F‴) Single confocal section of a stage 16 embryo expressing CD8-GFP driven by *sr-GAL4*, labeled for Robo2 and GFP. Arrow indicates tendon cells. (G-I′) Rescue of the *robo2* mutant muscle phenotype; all embryos are at stage 16. The LT muscles labeled with anti-Tropomyosin (G-I) or the DA3 muscle labeled with anti-Collier (G′-I′) are shown in embryos mutant for *robo2* (G,G′), embryos overexpressing Robo2 driven by *Mef2-GAL4* (H,H′), or embryos mutant for *robo2* overexpressing Robo2 in muscles (I,I′). (J,K) Knockdown of Robo2 with *sr-GAL4* in *robo2*$^{+/-}$ heterozygous embryos (K) compared with *robo2*$^{+/-}$ alone (J). (L) Quantification of D_{LT3}/D_s in the various mutant combinations as well as following rescue with *69B>Robo2*, *sr>Slit-UC-myc* and *sr>N-Slit-GFP*. Error bars indicate s.e.m. Horizontal lines show the span of the LT muscles 1-3. Scale bars: 10 μm.

CD8-GFP driven by the *sr-GAL4* driver (Fig. 2F′-F‴) verified the ectodermal expression of Robo2 at the surfaces of the tendon cells (open arrows in Fig. 2D-F and white arrows in Fig. 2F′-F‴). The relatively high ectodermal expression of Robo2-HA and its lack of staining in the affected LT and DA3 muscles were consistent with a muscle non-autonomous function of Robo2 in mediating LT and DA3 muscle patterning.

To address whether undetectable Robo2 protein was functioning in the muscles, we tested the ability of Robo2 to rescue the *robo2* mutant muscle phenotype when expressed in muscles. Driving Robo2 expression in muscles of *robo2* mutant embryos using the *Mef2-GAL4* driver did not rescue the muscle phenotype, but rather worsened the muscle pattern in all embryos tested as compared with WT embryos overexpressing Robo2 (Fig. 2G-I′). By contrast,

Development (2015) 142, 3512-3518 doi:10.1242/dev.128157

knockdown of Robo2 in tendons of *robo2*$^{-/+}$ heterozygous embryos (using *sr-GAL4>robo2 RNAi*) led to a phenotype similar to that of the *robo2* mutant; the LT muscles were mispatterned in 84% of the segments, and the DA3 muscle was aberrant in 31% of the segments (Fig. 2J-L; *robo2*$^{+/-}$*,sr>robo2i* versus WT, P=0.0001). Importantly, partial rescue of the LT muscle pattern was achieved by expressing Robo2 in the ectoderm using the *69B-GAL4* driver (Fig. 2L; *robo2;69B>Robo2* versus *robo2*, P=0.0001). Moreover, embryos in which *robo1* has been inserted into the *robo2* locus (Spitzweck et al., 2010) rescued the *robo2* muscle phenotype (data not shown), supporting the crucial contribution of Robo2's unique ectodermal distribution rather than its signaling activity.

In summary, the ectodermal expression of Robo2, its knockdown in tendons, and the ectodermal rescue imply that Robo2 functions in the ectoderm to induce the correct muscle pattern.

Robo2 enhances Slit cleavage

Next, we addressed the requirement for Slit in the ectodermal activity of Robo2, as associated with guiding the LT and DA3 muscles. We found strong genetic interaction between *robo2* and *slit* in inducing the LT and DA3 muscle pattern (Fig. 3A-C′). Trans-heterozygous embryos for both *robo2* and *slit* exhibited an aberrant pattern of LT muscles in 82% of the segments relative to 0% or 10% in *robo2*$^{-/+}$ or *slit*$^{-/+}$ embryos, respectively (P=0.0001). In the DA3 muscle, 10% of the segments of the trans-heterozygous *slit* or *robo2* embryos exhibited aberrant muscle orientation, in contrast to 0% in either of the single heterozygous mutants (P=0.0001). These results imply that Robo2 activity is mediated through its ligand Slit.

Next, we tested whether Robo2 affects Slit cleavage, which is crucial to short-range Slit signaling (Ordan et al., 2015). We overexpressed Robo2 in the entire embryonic ectoderm using the *69B-GAL4* driver and followed endogenous Slit cleavage by western blotting using an antibody that is reactive to the C-terminus of Slit; this antibody recognizes both full-length Slit (Slit-FL, ~170 kDa) and the C-terminal cleaved polypeptide (Slit-C, ~80 kDa). Strikingly, overexpression of Robo2 in the ectoderm led to an average 9.7-fold increase in the ratio of Slit-C relative to Slit-FL levels (P<0.05), implicating Robo2 in promoting Slit cleavage in the ectoderm (Fig. 3D,D′). By contrast, overexpression of Robo2 in the muscles (using the *Mef2-GAL4* driver) did not have

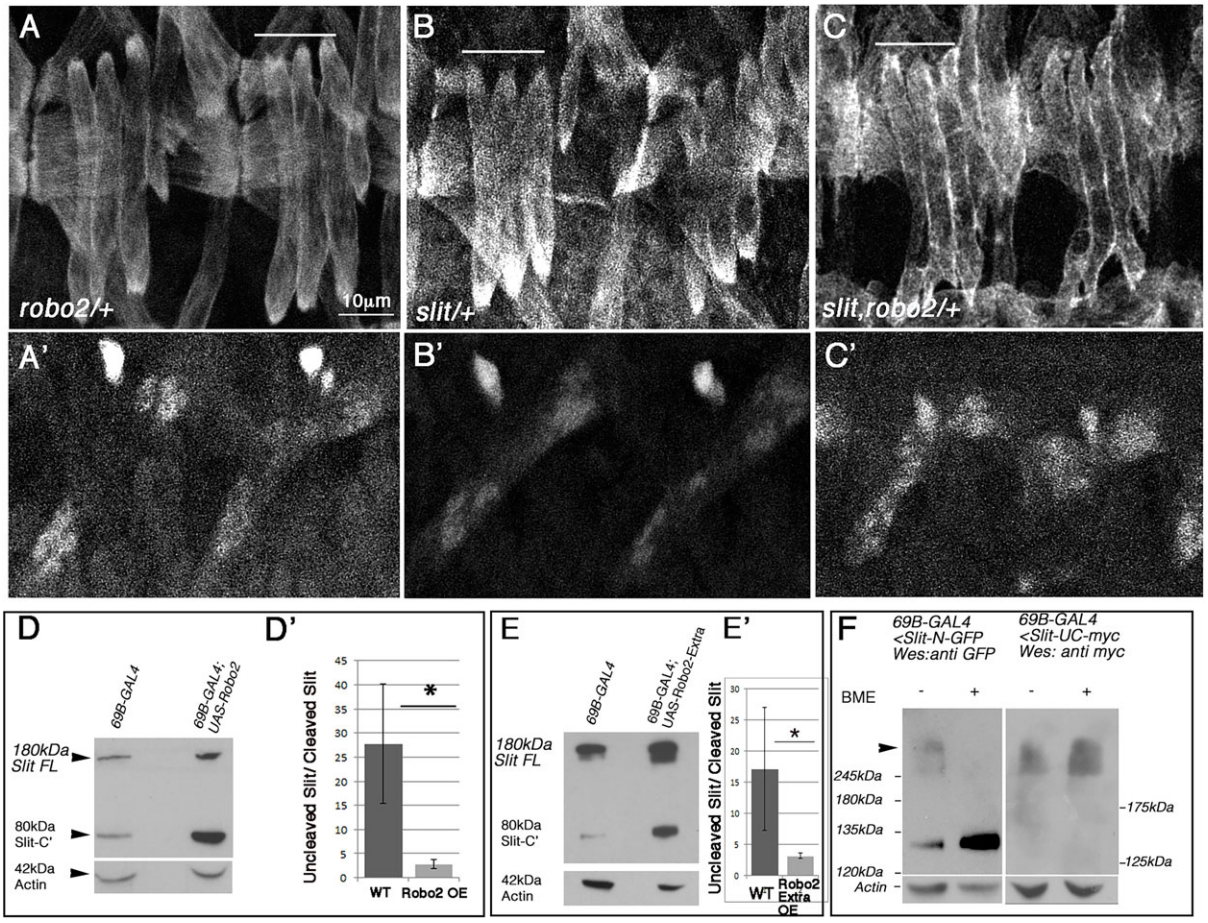

Fig. 3. Robo2 activity induces cleavage of Slit. (A-C′) Stage 16 embryos showing the LT and DA3 muscles of *robo2*$^{+/-}$ (A,A′), *slit*$^{+/-}$ (B,B′) or *robo2*$^{+/-}$*,slit*$^{+/-}$ (C,C′) embryos, visualized by anti-Tropomyosin (A-C) or anti-Collier (A′-C′). Horizontal lines indicate the span of LT muscles 1-3. Scale bar: 10 μm. (D) Representative western blot of five independent experiments of embryonic protein extract prepared from WT embryos (left lane) or from embryos at a similar developmental stage overexpressing Robo2 using the *69B-GAL4* driver (right lane), reacted with anti-Slit-C antibodies. Intact Slit (~175 kDa) and the cleaved Slit-C (80 kDa) are detected, but Slit-C levels are elevated in embryos overexpressing Robo2 relative to the control. The protein load in each extract is shown by anti-actin. (D′) The ratio between cleaved and uncleaved Slit in WT and in Robo2-overexpressing (OE) embryos. On average, Robo2 overexpression in the ectoderm induced a 9.7-fold elevation of cleaved Slit-C. (E) Representative western analysis with anti-Slit, similar to that in D except that the embryos carried Robo2 lacking the cytoplasmic domain. (E′) Quantification of the results shown in E representing three repetitions of the experiment. Error bars in D′ and E′ represent s.e.m., *P<0.0001. (F) Western blot of protein extract from embryos overexpressing either Slit-N-GFP or Slit-UC-myc performed in non-reducing (– BME) or reducing (+ BME) conditions, reacted with either anti-GFP or anti-myc. The protein load in each extract is shown by anti-actin. Arrowhead indicates Slit-N oligomer.

Development (2015) 142, 3512-3518 doi:10.1242/dev.128157

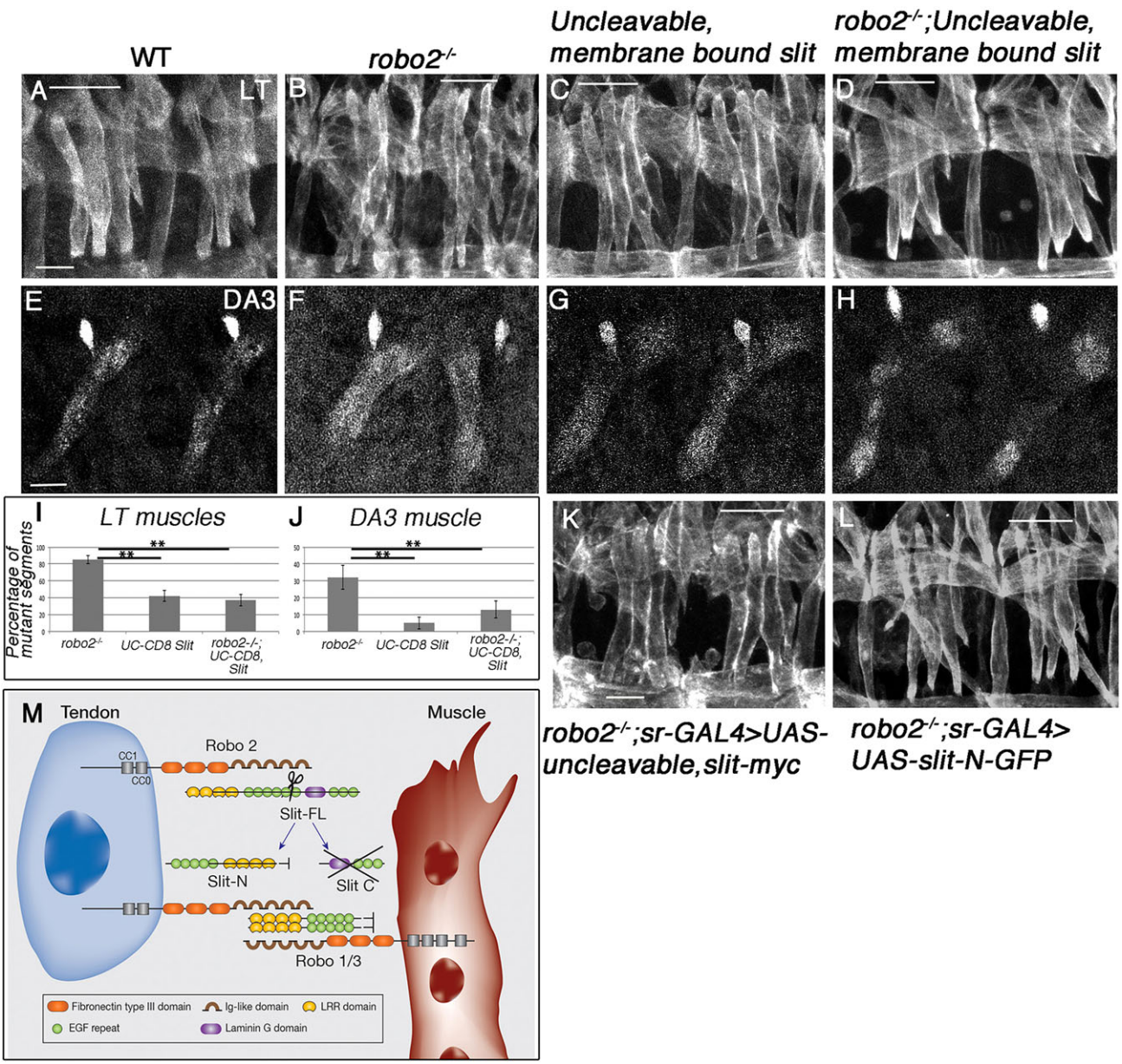

Fig. 4. Uncleavable membrane-bound Slit or secreted Slit-N rescues the *robo2* muscle phenotype. (A-H) Orientation of the LT muscles of stage 16 embryos visualized with anti-Tropomyosin (A-D) or of the DA3 muscle labeled with anti-Collier (E-H) in WT (A,E), *robo2* mutant (B,F), uncleavable membrane-bound knocked-in Slit (C,G) or *robo2;Slit-UC-CD8* double mutants (D,H). (I,J) Quantification of the data shown in A-H. Error bars represent s.e.m., $^{**}P<0.0001$. (K,L) The LT muscle phenotype in stage 16 *robo2* mutant embryos overexpressing Slit-UC-myc (K) or UAS-Slit-N-GFP (L), each driven by *sr-GAL4*. Horizontal lines indicate the span of LT muscles 1-3. Scale bars: 10 µm. (M) Model for the function of Robo2 activity in tendons in promoting the formation of Slit-N, which then forms oligomers bound to Robo2 on the tendon side and triggering Robo1/Robo3 signaling on the muscle side.

this effect (not shown). Remarkably, similarly enhanced Slit cleavage was observed following overexpression of truncated Robo2 lacking the cytoplasmic domain (Evans and Bashaw, 2010) (Fig. 3E,E′). Notably, overexpression of Robo1 in the ectoderm similarly enhanced Slit cleavage (data not shown). These results implicated a non-signaling function for Robo2 in promoting Slit cleavage.

We reasoned that covalently bound Slit oligomers, shown to form by previous crystallographic studies (Seiradake et al., 2009), would enable Slit to bind both of the juxtaposing Robo receptors – on the muscle side (Robo1 and/or Robo3) and on the tendon side (Robo2). We therefore tested for Slit oligomerization in embryos. Overexpression of either GFP-tagged cleaved Slit-N (Slit-N-GFP) or uncleavable full-length Slit-UC-myc was induced in the embryonic ectoderm with the *69B-GAL4* driver. The embryo extracts were then boiled under reducing [with β-mercaptoethanol (BME)] or non-reducing (without BME) conditions, separated on SDS-PAGE and analyzed by western blot using anti-GFP or anti-myc. Slit-N-GFP exhibited slower electrophoretic mobility in non-reducing than in reducing conditions (expected to be 124 kDa), supporting the formation of Slit-N-GFP oligomers by disulfide bonds (Fig. 3F, left panel). By contrast, Slit-UC-myc did not exhibit differential electrophoretic mobility in native versus denaturing conditions (Fig. 3F, right panel). This result is consistent with the unique ability of Slit-N to oligomerize.

Development (2015) 142, 3512-3518 doi:10.1242/dev.128157

Taken together, these results suggest that Robo2 in tendons enhances Slit cleavage, producing Slit-N oligomers at the tendon cell membrane that are potentially capable of binding both Robo2 in cis and Robo1/Robo3 in trans, leading to the spatial restriction of Slit signaling to the elongating muscle.

Knocked-in, membrane-bound, full-length Slit bypasses the requirement for Robo2

We reasoned that if the primary function of Robo2 is to promote localized Slit-N oligomers, then the knocked-in, membrane-bound, uncleavable Slit (Slit-UC-CD8) would rescue the phenotype of *robo2*. We therefore recombined knocked-in Slit-UC-CD8 [described by Ordan et al. (2015)] with *robo2* and analyzed the phenotype of the DA3 and LT muscles in homozygous embryos. Whereas in *robo2* mutants the orientation of the LT muscles was defective in 85% of the segments (Fig. 4A,B), the addition of knocked-in Slit-UC-CD8 showed only 37% defective segments (P=0.0001, n=46; Fig. 4D). Likewise, the D_{LT3}/D_s ratio was rescued (0.3±0.06 in the *robo2; Slit-UC-CD8* embryos relative to 0.16±0.1 in *robo2*, P=0.015). Given that Slit-UC-CD8 by itself produced a moderate muscle phenotype (Fig. 4C), we concluded that Slit-UC-CD8 is capable of rescuing the *robo2* phenotype of the LT muscles (Fig. 4I). For the DA3 muscle, whereas 32% of the segments showed a phenotype in *robo2* mutants, *robo2* mutant embryos recombined with Slit-UC-CD8 showed a muscle phenotype in only 13% of the segments (P=0.035), and Slit-UC-CD8 mutants showed only 5% defective segments (Fig. 4E-H,J).

Moreover, consistent with a major function of Robo2 in promoting Slit cleavage, overexpression of the active cleaved Slit-N-GFP in tendon cells rescued the *robo2* mutant LT muscle phenotype in 73% of the segments (Fig. 4L and Fig. 2L; *robo2; sr>Slit-N* versus *robo2*, P=0.0001), whereas expression of Slit-UC-myc alone did not (Fig. 4K and Fig. 2L; *robo2;sr>Slit-UC* versus *robo2*, P=0.9268). These results are consistent with a major function for Robo2 in promoting Slit-N accumulation at the tendon cell membrane, presumably by retaining Slit-FL and enhancing its availability for proteolytic cleavage. Slit-N oligomers potentially bind to both Robo2 at the tendon side as well as to Robo1 and/or Robo3 at the muscle side to promote a unidirectional short-range Slit-repulsive signal in muscles (Fig. 4M). In this context the Robo2 cytoplasmic signaling domain is dispensable, consistent with Robo2 function in chordotonal organs (Kraut and Zinn, 2004) and with Robo2 non-autonomous function in the CNS (Evans et al., 2015).

In conclusion, our findings demonstrate a novel, non-signaling role for Robo2 in tendons in regulating the local distribution of active cleaved Slit oligomers at the tendon cell membrane. This signal is crucial in promoting the Slit short-range signaling in muscles that is essential for directional muscle elongation. Such a mechanism might be significant in other setups in which Slit promotes signaling between neighboring cells.

MATERIALS AND METHODS

Fly strains

Wild-type flies were of the *yw* strain. The strains *robo2[4]*, *robo2[8]*, *robo2→robo1* (*robo1* knocked into *robo2*), *robo3[1]*, Slit-UC-CD8 (uncleavable membrane-bound Slit/CyO Wg-lacZ), Robo1-HA knock-in, Robo2-HA knock-in, Robo3-HA knock-in and UAS-Robo2-HA were produced by the B. J. Dickson lab (Janelia Research Campus, Ashburn, VA, USA). *Mef2-GAL4*, *69B-GAL4*, sli^2*/CyO,Yfp* $robo^1$*/CyO,Yfp* and *robo2* RNAi flies were obtained from Bloomington *Drosophila* Stock Center, Indiana University. Stripe-GAL4 flies were provided by G. Morata (CBMSO, Universidad Autonoma de Madrid, Madrid, Spain). Collier-GFP flies were a gift from Dr Alan Vincent (Centre de Biologie du Développement, UMR 5547 and IFR 109, CNRS and Université Paul Sabatier) (Dubois et al., 2007; Enriquez et al., 2012). Homozygous embryos were recognized by the lack of either CyO,YFP or CyO,Wg-lacZ. UAS-slit-N-GFP and UAS-U-slit-myc and UAS-Robo2-Extra strains were a gift of Greg J. Bashaw (Coleman et al., 2010). Ap-Me580-GFP flies were a gift of Mary Baylies (Folker et al., 2012, 2014). $slit^2$ and *robo2[8]* and Slit uncleavable (Slit-UC) and *robo2[8]* were recombined by conventional methods.

Antibodies

Mouse anti-Collier (Knot) antibody (1:200) was produced by the Alan Vincent lab (Centre de Biologie du Développement). Additional antibodies included rat anti-Tropomyosin (1:400; Abcam, Ab-50567), goat polyclonal anti-myc (1:1000; Abcam, ab9132), mouse anti-GFP (1:200; Roche, 1184460001), chick anti-β-gal (1:400; Abcam, 9361), chick anti-GFP (1:400; Aves Labs, GFP-1020), guinea pig anti-Stripe (1:400; produced in the T.V. lab), rabbit anti-Robo2 (1:200; produced by B. J. Dickson), chick anti-HA (1:400; Aves Labs, ET-HA100), mouse anti-HA (1:400; Covance, MMs-101p), mouse anti-myc (1:60; Developmental Studies Hybridoma Bank, 9E10) and mouse anti-Slit (1:30; Developmental Studies Hybridoma Bank, The University of Iowa). Secondary fluorescent antibodies were purchased from Jackson Laboratories.

Immunostaining

Staged embryos were collected and fixed as previously described (Ashburner et al., 2005). Embryos were visualized with a Zeiss LSM710 confocal microscope and images were processed using Adobe Photoshop.

Live imaging

Staged embryos were dechorionated and balancer was recognized using a fluorescent stereoscope. Then, embryos were placed on a piece of agar glued to a coverslip with 3 M glue, covered with Halocarbon oil 700 (Sigma-Aldrich, H8898), and visualized with a Zeiss LSM710/780 confocal microscope. Images were deconvoluted using AutoQuant (Media Cybernetics, AutoQuant X3) and time series were transformed into a film using ImageJ (NIH).

Western blot

Protein extract was produced from staged embryos in RIPA buffer. Extract was boiled in sample buffer with or without BME and run on a 7% SDS-PAGE gel, blotted onto nitrocellulose and reacted with mouse anti-Slit antibody (1:1000; Developmental Studies Hybridoma Bank) and HRP-conjugated anti-mouse IgG (1:5000; Jackson ImmunoResearch, 715-035-151). The signal was visualized using SuperSignal (Thermo Scientific). Film was scanned and relative band intensities were measured using ImageJ. Statistical significance was determined by the Mann-Whitney U-test.

Statistical analysis

Segments were scored separately, and the fraction of mutant segments for each genetic background was calculated. The significance of the effect was calculated using the following test:

$$Z=\frac{\hat{\pi}_1-\hat{\pi}_2}{\sigma_{\hat{\pi}_1-\hat{\pi}_2}} \text{ and } \sigma_{\hat{\pi}_1-\hat{\pi}_2}=\sqrt{\pi(1-\pi)\left(\frac{1}{n_1}+\frac{1}{n_2}\right)}.$$

Acknowledgements

We thank A. Vincent, M. Baylies and B. Dickson for gifts of antibodies and/or flies, the Bloomington Stock Center for fly lines, and the Developmental Studies Hybridoma Bank for antibodies. We also thank N. Konstantin for corrections to the manuscript.

Competing interests

The authors declare no competing or financial interests.

Development (2015) 142, 3512-3518 doi:10.1242/dev.128157

Author contributions

E.O. and T.V. developed the concepts; E.O. performed the experiments and data analysis; T.V. and E.O. wrote the manuscript.

Funding

This study was supported by the Israeli Science Foundation (ISF) [grant number 71/12 to T.V.].

Supplementary information

Supplementary information available online at
http://dev.biologists.org/lookup/suppl/doi:10.1242/dev.128157/-/DC1

References

Ashburner, M., Golic, K. G. and Hawley, R. S. (2005). *Drosophila: A Laboratory Handbook*, 2nd edn. Cold Spring Harbor, N.Y: Cold Spring Harbor Laboratory Press.

Brose, K., Bland, K. S., Wang, K. H., Arnott, D., Henzel, W., Goodman, C. S., Tessier-Lavigne, M. and Kidd, T. (1999). Slit proteins bind Robo receptors and have an evolutionarily conserved role in repulsive axon guidance. *Cell* **96**, 795-806.

Coleman, H. A., Labrador, J.-P., Chance, R. K. and Bashaw, G. J. (2010). The Adam family metalloprotease Kuzbanian regulates the cleavage of the roundabout receptor to control axon repulsion at the midline. *Development* **137**, 2417-2426.

Dubois, L., Enriquez, J., Daburon, V., Crozet, F., Lebreton, G., Crozatier, M. and Vincent, A. (2007). Collier transcription in a single Drosophila muscle lineage: the combinatorial control of muscle identity. *Development* **134**, 4347-4355.

Enriquez, J., de Taffin, M., Crozatier, M., Vincent, A. and Dubois, L. (2012). Combinatorial coding of Drosophila muscle shape by Collier and Nautilus. *Dev. Biol.* **363**, 27-39.

Evans, T. A. and Bashaw, G. J. (2010). Functional diversity of Robo receptor immunoglobulin domains promotes distinct axon guidance decisions. *Curr. Biol.* **20**, 567-572.

Evans, T. A., Santiago, C., Arbeille, E. and Bashaw, G. J. (2015). Robo2 acts in trans to inhibit Slit-Robo1 repulsion in pre-crossing commissural axons. *eLife* **4**, e08407.

Folker, E. S., Schulman, V. K. and Baylies, M. K. (2012). Muscle length and myonuclear position are independently regulated by distinct Dynein pathways. *Development* **139**, 3827-3837.

Folker, E. S., Schulman, V. K. and Baylies, M. K. (2014). Translocating myonuclei have distinct leading and lagging edges that require kinesin and dynein. *Development* **141**, 355-366.

Kramer, S. G., Kidd, T., Simpson, J. H. and Goodman, C. S. (2001). Switching repulsion to attraction: changing responses to slit during transition in mesoderm migration. *Science* **292**, 737-740.

Kraut, R. and Zinn, K. (2004). Roundabout 2 regulates migration of sensory neurons by signaling in trans. *Curr. Biol.* **14**, 1319-1329.

Ordan, E., Brankatschk, M., Dickson, B., Schnorrer, F. and Volk, T. (2015). Slit cleavage is essential for producing an active, stable, non-diffusible short-range signal that guides muscle migration. *Development* **142**, 1431-1436.

Schejter, E. D. and Baylies, M. K. (2010). Born to run: creating the muscle fiber. *Curr. Opin. Cell Biol.* **22**, 566-574.

Schnorrer, F. and Dickson, B. J. (2004). Muscle building; mechanisms of myotube guidance and attachment site selection. *Dev. Cell* **7**, 9-20.

Schweitzer, R., Zelzer, E. and Volk, T. (2010). Connecting muscles to tendons: tendons and musculoskeletal development in flies and vertebrates. *Development* **137**, 2807-2817.

Seiradake, E., von Philipsborn, A. C., Henry, M., Fritz, M., Lortat-Jacob, H., Jamin, M., Hemrika, W., Bastmeyer, M., Cusack, S. and McCarthy, A. A. (2009). Structure and functional relevance of the Slit2 homodimerization domain. *EMBO Rep.* **10**, 736-741.

Spitzweck, B., Brankatschk, M. and Dickson, B. J. (2010). Distinct protein domains and expression patterns confer divergent axon guidance functions for Drosophila Robo receptors. *Cell* **140**, 409-420.

Volk, T. (1999). Singling out Drosophila tendon cells: a dialogue between two distinct cell types. *Trends Genet.* **15**, 448-453.

Wang, K. H., Brose, K., Arnott, D., Kidd, T., Goodman, C. S., Henzel, W. and Tessier-Lavigne, M. (1999). Biochemical purification of a mammalian slit protein as a positive regulator of sensory axon elongation and branching. *Cell* **96**, 771-784.

Wayburn, B. and Volk, T. (2009). LRT, a tendon-specific leucine-rich repeat protein, promotes muscle-tendon targeting through its interaction with Robo. *Development* **136**, 3607-3615.

Movie 1. Time-lapse of live wild-type embryo at stages 13-16, in which the LT muscles are labeled with GFP (Ap-Me580-GFP).

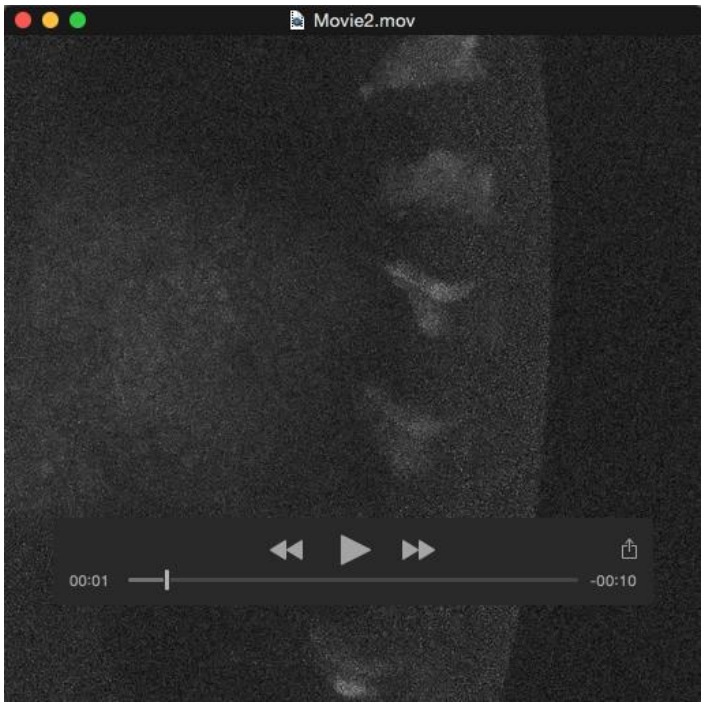

Movie 2. Time-lapse of live *robo2* mutant embryo at stages 13-16, in which the LT muscles are labeled with GFP (Ap-Me580-GFP).

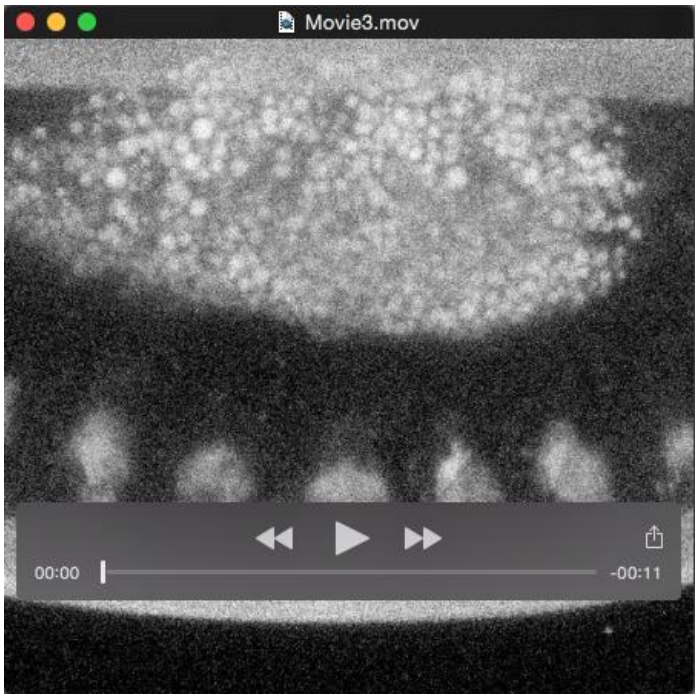

Movie 3. Time-lapse of live wild-type embryo at stages 13-16, in which the DA3 muscle is labeled with GFP (Collier-GFP).

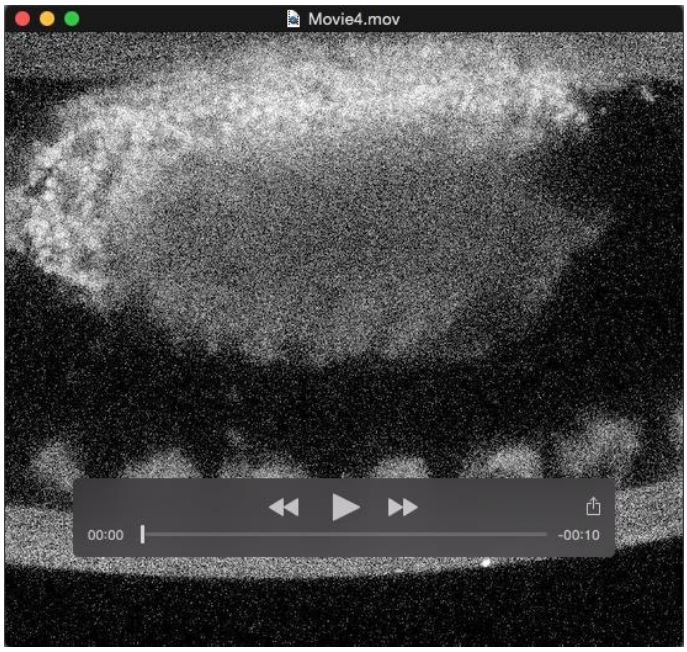

Movie 4. Time-lapse of live *robo2* mutant embryo at stages 13-16, in which the DA3 muscle is labeled with GFP (Collier-GFP).